

Direct production of three-color polarization entanglement for continuous variable

ZHIHUI YAN* AND XIAOJUN JIA

State Key Laboratory of Quantum Optics and Quantum Optics Devices, Institute of Opto-Electronics, Shanxi University, Taiyuan 030006, China
*Corresponding author: zhyan@sxu.edu.cn

Received 21 May 2015; revised 23 August 2015; accepted 24 August 2015; posted 26 August 2015 (Doc. ID 241470); published 16 September 2015

The direct generation of discrete-variable three-photon polarization entanglement has been recently demonstrated [Nat. Photonics 8, 801 (2014)]. Here, we propose a feasible scheme to generate continuous-variable (CV) three-color polarization entangled states of light in a deterministic way. The method initially prepares a tripartite quadrature entanglement based on two cascaded nondegenerate optical parametric oscillators. The entangled modes are then coupled, respectively, with three strong coherent optical beams on polarized beam splitters, leading to the generation of the three-color CV polarization entanglement. The polarization entanglement is then verified by inseparability criterion and positive partial transposition criterion. Additionally, optimal parameters in practical conditions are obtained through numerical simulations, which could provide useful guidance for experimental implementations. The demonstrated CV three-color polarization entanglement is suitable in quantum information processing tasks relying on the direct interaction between spin of atoms and polarization of light. © 2015 Optical Society of America

OCIS codes: (270.0270) Quantum optics; (190.4970) Parametric oscillators and amplifiers.

<http://dx.doi.org/10.1364/JOSAB.32.002139>

1. INTRODUCTION

Quantum entanglement is a central concept for quantum information technologies [1]. With the development of quantum information, various kinds of quantum-entangled states of light have been generated and applied in different quantum information protocols. Entangled photon pairs [2] and eight-photon entanglement [3] are generated by combining photons from two or more different spontaneous parametric downconversions (SPDCs). The Einstein–Podolsky–Rosen (EPR) entangled state [4] and eight partite entangled optical fields [5] are produced by interfering optical fields from two or more different optical parametric amplifiers (OPAs). Quantum internet, involving both matter and light, allows the distribution of entanglement to every node and the teleportation of quantum states between nodes across the quantum networks [6]. The atom is one of the suitable candidates of the quantum information processing and memory nodes due to good atomic coherence, and the storage and retrieval of light have been experimentally demonstrated based on rubidium and cesium atoms by many groups [7–15]. Meanwhile, the light is the best quantum information carrier as a result of the fast transmission speed and the weak interaction of the environment; thus, the quantum nodes can be connected by optical fibers. Multicolor entangled state of light with different frequencies is demanded in quantum internet to connect the quantum networking nodes and channels. The direct generation of three-photon entanglement with different frequencies in energy and

time has been experimentally realized using the nonlinear process of the cascaded SPDC system [16,17]. In the CV regime, a nondegenerate optical parametric oscillator (NOPO) above the threshold is one of the well-understood devices for producing a CV two-color quadrature entangled state [18–22]. Considering the quantum correlation among the reflected pump optical fields and downconverted signal and idler optical fields, CV three-color quadrature entanglement is theoretically and experimentally obtained in a single NOPO [23,24]. Another approach for generating three-color entanglement is based on the cascaded NOPO system consisting of two NOPOs. The resulting three downconverted optical beams are three-color quadrature entanglement in room temperature deterministically, and their wavelengths are 852 nm, corresponding to the cesium atomic absorption line, 1550 and 1440 nm, matching the optical fiber transmission window [25,26].

On the other hand, not only quadrature entanglement but also polarization entanglement has attracted extensive attention. Because light polarization described by Stokes vector on a Poincare sphere corresponds to atomic spin described by Stokes vector on a Bloch sphere, the polarization of light can directly interact with the spin of the atom, which is a potential candidate for the quantum interface of atoms and light [15]. In the past years, the DV photon polarization state in the quantum mechanical regime of photon pairs or even eight photons with the same wavelength has been widely researched [2,3]. In

2014, DV three-color polarization entanglement with different wavelengths was directly generated by a cascaded photon pair polarization entanglement source, and their wavelengths can be suitable for quantum communication [27]. Comparatively, the CV polarization state has received much attention, and Korolkova *et al.* introduced the concept of the CV polarization entanglement [28]. Thus, the CV polarization of light can be used in quantum memory and long distance quantum communication [15,29]. Further, the bipartite polarization entanglement of optical fields is experimentally designed to transform the quadrature entanglement to polarization entanglement produced by OPAs [15,30]. Polarization entanglement is also produced with an asymmetric fiber-optic Sagnac interferometer and a cloud of cold cesium atoms in a high-finesse optical cavity [28,31]. All the above CV bipartite polarization entangled optical fields are with the same wavelength, and the research on the CV multicolor polarization entanglement with different wavelengths is also crucially important for the quantum information networks, which has not been reported thus far.

In this paper, we propose direct generation of CV three-color Greenberger–Horne–Zeilinger-like (GHZ-like) polarization entanglement, and the main point is that the tripartite polarization entangled optical beams with different wavelengths are generated and can be applied in quantum networks, consisting of cesium atom quantum nodes and optical fiber quantum channels. The resulting multicolor polarization entanglement source is one kind of fundamental resource for storage and retrieval of the quantum state and long-distance quantum communication. For example, in balanced homodyne detection of the quadrature, the phase-locking fluctuation between the signal optical beam and local oscillation is large after they pass the atomic memory medium or long-distance optical fiber, respectively. Fortunately, this problem can be solved by using the light polarization for quantum memory or quantum communication because local oscillation free measurement can overcome the above fluctuation of phase locking. By combining the techniques of a cascaded NOPO system, which consists of two NOPOs and coupling of the coherent state with quadrature entanglement, we can produce three-color polarization entanglement containing the advantages of not only connecting the quantum nodes and channels but also effective interaction and measurement. The entanglement criterion is required for the generalizing of three-color polarization entanglement. According to the inseparability criterion [32,33] and PPT criterion [34,35] for quadrature entanglement and the commutation relation of light polarization, we have obtained the three-color inseparability criterion and PPT criterion for polarization entangled optical fields. The generalizing of multipartite polarization entanglement requires critical conditions, such as the optimal structure and parameters of system. The dependence of the correlation variance and the smallest symplectic eigenvalues of the partial transposition covariance matrix of the three optical beams on the experimental parameters of the cascaded NOPO system are analyzed, and we obtain the optimal pump power factor and transmissivity of the pump input coupler and the signal (idler) output coupler of the two NOPOs according to the numerical calculation and practical experimental conditions. This provides a direct reference for the design of experimental systems.

Four features of the proposal should be emphasized. First, this approach can create three-color polarization entanglement deterministically, without the need for the post-selection, and can be useful for application in many quantum information protocols. Second, the wavelengths of the CV three-color polarization entangled optical fields from this source can be easily tuned by precisely controlling the temperature of the nonlinear crystal due to NOPO's well-known tunable advance, which can be applied in quantum information networks containing atomic quantum memory and optical fiber quantum communication. Third, the polarization entangled optical fields can directly interact with the atom and are useful for the quantum interface between light and atom [15] and the quantum networks [6]. Finally, the measurement of light polarization does not need the local oscillation [29].

In the following, we will describe the cascaded NOPO system and generate the CV three-color GHZ-like quadrature entanglement based on the Langevin equation, thus describing the evolution of quantum fluctuation of optical fields from NOPO in Section 2. Then, the transformation of quadrature entanglement to the polarization entanglement is demonstrated in Section 3. In Section 4, we verify the CV three-color polarization entangled optical fields by means of inseparability criterion and PPT criterion, respectively. We further obtain the optimal experimental parameters of the cascaded NOPO system by numerical analysis. Finally, a brief conclusion is shown in Section 5.

2. SCHEMATIC OF CASCADED NOPO SYSTEM

In our proposal, the CV three-color spatially separated Greenberger–Horne–Zeilinger-like (GHZ-like) polarization entangled state of optical fields is directly generated by coupling strong coherent optical fields with weak CV three-color quadrature polarization entanglement from a cascaded NOPO system consisting of two NOPOs. The setup is demonstrated in Fig. 1. We first prepare a three-color quadrature entangled state from a cascaded NOPO system and then transform it into three-color polarization entanglement. The primary NOPO is pumped by coherent optical fields \hat{a}_1 at wavelength λ_1 to produce the optical fields \hat{a}_2 and \hat{a}_3 at wavelengths λ_2 and λ_3 . At the same time, the pump optical fields of the secondary NOPO are from the optical fields \hat{a}_3 , one of the output entangled optical beams from the primary NOPO. The secondary NOPO generates optical fields \hat{a}_4 and \hat{a}_5 at wavelengths λ_4 and λ_5 , respectively. The resulting quantum state of three optical beams will be a three-color GHZ-like quadrature entangled state because one of the downconverted optical fields \hat{a}_3 from

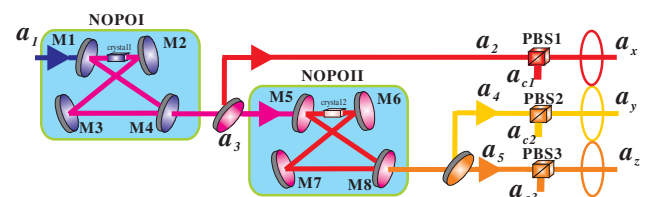


Fig. 1. Schematic of CV three-color polarization entangled optical fields using cascaded NOPO system.

the primary NOPO is used as the pump optical fields of the secondary NOPO, and its quantum correlations with the other downconverted optical fields \hat{a}_2 from the primary NOPO will directly be coupled into the signal and the idler optical fields \hat{a}_4 and \hat{a}_5 of the secondary NOPO through an intracavity nonlinear interaction. The resulting quantum state of three optical beams will be a three-color GHZ-like quadrature entangled state. Then, we can transform quadrature entanglement to polarization entanglement by coupling strong coherent light \hat{a}_{1c} , \hat{a}_{2c} , and \hat{a}_{3c} , with weak quadrature entangled optical fields \hat{a}_2 , \hat{a}_4 , and \hat{a}_5 , on PBS1, PBS2, and PBS3. The final output optical fields \hat{a}_x , \hat{a}_y , and \hat{a}_z are CV three-color GHZ-like polarization entangled state of optical fields.

In quantum optics, optical fields are represented by annihilation operator \hat{a} , and the amplitude \hat{X} and phase \hat{Y} quadratures correspond to the real and imaginary parts of the annihilation \hat{a} , as $\hat{X} = \hat{a} + \hat{a}^\dagger$, $\hat{Y} = (\hat{a} - \hat{a}^\dagger)/i$. In CV regimes, NOPO operating above the threshold is a well-understood tool for generating bright quadrature entangled optical fields; this tool is also tunable by changing the temperature of the nonlinear crystal. The entanglement exists between the downconverted signal and idler optical fields. The NOPOI (II), as shown in Fig. 1, is pumped by frequency $\omega_{1(3)}$ optical fields to generate signal and idler optical fields with frequencies $\omega_{2(4)}$ and $\omega_{3(5)}$. Due to the conservation of energy in the intracavity frequency downconversion process, the frequencies of the pump, signal, and idler optical fields satisfy the relations $\omega_{1(3)} = \omega_{2(4)} + \omega_{3(5)}$. Conservation of momentum in this process is known as phase matching. Each NOPO employs a bow-tie-type ring configuration in order to exclude the influence of backpropagating light from the NOPOII. Each NOPO is composed of a nonlinear crystal, two spherical mirrors $M_{1(5)}$ and $M_{2(6)}$, and two flat mirrors $M_{3(7)}$ and $M_{4(8)}$, and the three intracavity modes of signal $\hat{a}_{2(4)}$, idler $\hat{a}_{3(5)}$, and pump $\hat{a}_{1(3)}$ optical fields resonate simultaneously. For pump optical fields of each NOPO, the input coupling mirrors have the same transmissivity $\gamma_{1(3)}$, introducing the input vacuum noise $\hat{a}_{\alpha 1(3)}^{\text{in}}$, and all the other three-cavity mirrors are highly reflective. The intracavity loss of the optical components is $\mu_{1(3)}$, producing the intracavity loss noise $\hat{a}_{\beta 1(3)}^{\text{in}}$. The total loss of the pump optical fields for each NOPO is $\gamma'_{1(3)} = \gamma_{1(3)} + \mu_{1(3)}$. We assume all the parameters are the same for the signal and idler optical fields of each NOPO, which are resonant with the cavity. The output couplers of signal and idler fields have the same transmissivity $\gamma_{2(4)}$, thus introducing the input vacuum noise $\hat{a}_{\alpha 2(4)}^{\text{in}}$ and $\hat{a}_{\alpha 3(5)}^{\text{in}}$, and all the other three cavity mirrors are highly reflective. The intracavity loss of the optical components is $\mu_{2(4)}$, producing the intracavity loss noise $\hat{a}_{\beta 2(4)}^{\text{in}}$ and $\hat{a}_{\beta 3(5)}^{\text{in}}$. Therefore, the total loss of the signal and idler optical fields for each NOPO is $\gamma'_{2(4)} = \gamma_{2(4)} + \mu_{2(4)}$. The cavity mirror $M_{3(7)}$ is mounted on a PZT_{1(2)}} for scanning or locking the cavity length of the NOPO to the resonance with the signal (idler) optical fields. The pump power factor is defined as $\sigma_{1(2)} = \sqrt{P_{1(2)}/P_{th1(2)}}$, where $P_{1(2)}$ is the input pump power and $P_{th1(2)}$ is the pump threshold power of each NOPO.

We use the Langevin equations of operators to describe the evolution of quantum fluctuation of optical modes from NOPO, which is equivalent to the Fokker–Planck equations deriving from the density operator master equation. By linearizing process and just considering the quantum fluctuation $\delta\hat{x}_i = \hat{x}_i - \langle\hat{x}_i\rangle$, the Langevin equations is shown as

$$\frac{d}{dt}\hat{X}_{1(2)} = \hat{M}_{A_{1(2)}}\hat{X}_{1(2)} + \hat{M}_{\gamma_{1(2)}}\hat{X}_{\alpha 1(2)}^{\text{in}} + \hat{M}_{\mu_{1(2)}}\hat{X}_{\beta 1(2)}^{\text{in}}. \quad (1)$$

In the linearizing description, $\hat{X}_{1(2)}$ represents the quantum fluctuations of the amplitude and phase quadratures of the pump, signal, and idler optical fields inside the NOPOI(II), which can be expressed as

$$\hat{X}_{1(2)} = [\delta\hat{x}_{1(3)}, \delta\hat{y}_{1(3)}, \delta\hat{x}_{2(4)}, \delta\hat{y}_{2(4)}, \delta\hat{x}_{3(5)}, \delta\hat{y}_{3(5)}]^T. \quad (2)$$

And $\hat{X}_{\alpha 1(2)}^{\text{in}}$ means the amplitude and phase quadratures vacuum fluctuation into the NOPOI(II) through the pump input coupler and signal and idler output coupler, expressed as

$$\hat{X}_{\alpha 1(2)}^{\text{in}} = [\delta\hat{x}_{\alpha 1(3)}^{\text{in}}, \delta\hat{y}_{\alpha 1(3)}^{\text{in}}, \delta\hat{x}_{\alpha 2(4)}^{\text{in}}, \delta\hat{y}_{\alpha 2(4)}^{\text{in}}, \delta\hat{x}_{\alpha 3(5)}^{\text{in}}, \delta\hat{y}_{\alpha 3(5)}^{\text{in}}]^T. \quad (3)$$

And $\hat{X}_{\beta 1(2)}^{\text{in}}$ characterizes the amplitude and phase quadratures vacuum fluctuation into the NOPOI(II) from the intracavity loss, shown as

$$\hat{X}_{\beta 1(2)}^{\text{in}} = [\delta\hat{x}_{\beta 1(3)}^{\text{in}}, \delta\hat{y}_{\beta 1(3)}^{\text{in}}, \delta\hat{x}_{\beta 2(4)}^{\text{in}}, \delta\hat{y}_{\beta 2(4)}^{\text{in}}, \delta\hat{x}_{\beta 3(5)}^{\text{in}}, \delta\hat{y}_{\beta 3(5)}^{\text{in}}]^T. \quad (4)$$

Here, $\hat{M}_{A_{1(2)}}$ stands for the drift matrix for NOPOI(II), describing the interaction of the three modes in the cavity, demonstrated as

$$\hat{M}_{A_{1(2)}} = \begin{pmatrix} -m_1 & 0 & -m_3 & 0 & -m_3 & 0 \\ 0 & -m_1 & 0 & -m_3 & 0 & -m_3 \\ m_3 & 0 & -m_2 & 0 & m_2 & 0 \\ 0 & m_3 & 0 & -m_2 & 0 & -m_2 \\ m_3 & 0 & m_2 & 0 & -m_2 & 0 \\ 0 & m_3 & 0 & -m_2 & 0 & -m_2 \end{pmatrix}, \quad (5)$$

where $m_1 = \gamma'_{1(3)}$, $m_2 = \gamma'_{2(4)}$, and $m_3 = \sqrt{\gamma'_{1(3)}\gamma'_{2(4)}}(\sigma_{1(2)} - 1)$.

And $\hat{M}_{\gamma_{1(2)}}$ is the matrix for NOPOI(II) describing the coupling of vacuum noise by the pump input and signal (idler) output coupling mirrors:

$$\hat{M}_{\gamma_{1(2)}} = \text{diag}[m_4, m_4, m_5, m_5, m_5, m_5], \quad (6)$$

where $m_4 = \sqrt{2\gamma_{1(3)}}$, $m_5 = \sqrt{2\gamma_{2(4)}}$.

And $\hat{M}_{\mu_{1(2)}}$ is the matrix for NOPOI(II) corresponding to the loss coefficients of all the optical components:

$$\hat{M}_{\mu_{1(2)}} = \text{diag}[m_6, m_6, m_7, m_7, m_7, m_7], \quad (7)$$

where $m_6 = \sqrt{2\mu_{1(3)}}$, $m_7 = \sqrt{2\mu_{2(4)}}$.

The input and output relation of NOPO is as follows:

$$\hat{X}_{1(2)}^{\text{out}} = \hat{M}_{\gamma_{1(2)}}\hat{X}_{1(2)} - \hat{X}_{\alpha 1(2)}^{\text{in}}. \quad (8)$$

According to the solution $\hat{X}_{1(2)}$ of the Langevin equation and the input and output relation of NOPO, we are able to obtain the analytical analysis of the amplitude and phase quadrature fluctuation $\hat{X}_{1(2)}^{\text{out}}$ of the output optical fields for pump, signal, and idler optical fields from the NOPO.

3. TRANSFORMATION OF CV QUADRATURE TO CV POLARIZATION OF LIGHT

The atomic spin state can be described as a Stokes vector on a Bloch sphere; similarly, the light polarization state can be described as a Stokes vector on a Poincare sphere. There are four Stokes operators for light: \hat{S}_0 represents light intensity and \hat{S}_1 , \hat{S}_2 , and \hat{S}_3 characterize horizontal, diagonal, and right circular polarizations, respectively. The following Stokes operators can be expressed by means of annihilation and creation operators of the horizontally and vertically polarized modes:

$$\begin{aligned}\hat{S}_0 &= \hat{a}_H^\dagger \hat{a}_H + \hat{a}_V^\dagger \hat{a}_V, \\ \hat{S}_1 &= \hat{a}_H^\dagger \hat{a}_H - \hat{a}_V^\dagger \hat{a}_V, \\ \hat{S}_2 &= \hat{a}_H^\dagger \hat{a}_V e^{i\theta} + \hat{a}_V^\dagger \hat{a}_H e^{-i\theta}, \\ \hat{S}_3 &= (\hat{a}_H^\dagger \hat{a}_V e^{i\theta} - \hat{a}_V^\dagger \hat{a}_H e^{-i\theta})/i,\end{aligned}\quad (9)$$

where θ is the phase difference between the H and V polarization modes. According to the commutation relations of annihilation and creation operators $[\hat{a}_k, \hat{a}_l] = \delta_{kl}$, ($k, l \in \{H, V\}$), the commutation relations of Stokes operators are as follows:

$$\begin{aligned}[\hat{S}_0, \hat{S}_j] &= 0, (j = 1, 2, 3) \\ [\hat{S}_1, \hat{S}_2] &= 2i\hat{S}_3, [\hat{S}_2, \hat{S}_3] = 2i\hat{S}_1, [\hat{S}_3, \hat{S}_1] = 2i\hat{S}_2,\end{aligned}\quad (10)$$

The value of the commutation relations of Stokes operators can be determined by the average values of the Stokes operators.

According to the definition of Stokes operators, they can be obtained from the quadratures of optical fields by combining the strong vertical polarization optical fields α_V and the weak horizontal polarization optical fields α_H on PBS. The mean values of Stokes operators are

$$\begin{aligned}\langle \hat{S}_0 \rangle &= \alpha_H^2 + \alpha_V^2, \\ \langle \hat{S}_1 \rangle &= \alpha_H^2 - \alpha_V^2, \\ \langle \hat{S}_2 \rangle &= 2\alpha_H \alpha_V \cos \theta, \\ \langle \hat{S}_3 \rangle &= 2\alpha_H \alpha_V \sin \theta.\end{aligned}\quad (11)$$

The quantum fluctuations of Stokes operators are

$$\begin{aligned}\Delta^2 \hat{S}_0 &= \Delta^2 \hat{S}_1 = \alpha_V^2 \Delta^2 \hat{X}_V + \alpha_H^2 \Delta^2 \hat{X}_H, \\ \Delta^2 \hat{S}_2(\theta=0) &= \Delta^2 \hat{S}_3(\theta=\pi/2) = \alpha_V^2 \Delta^2 \hat{X}_H + \alpha_H^2 \Delta^2 \hat{X}_V, \\ \Delta^2 \hat{S}_3(\theta=0) &= \Delta^2 \hat{S}_2(\theta=\pi/2) = \alpha_V^2 \Delta^2 \hat{Y}_H + \alpha_H^2 \Delta^2 \hat{Y}_V.\end{aligned}\quad (12)$$

In the following text, we choose the power of light in the vertical polarization direction, which is larger than that in the horizontal direction, as $\alpha_H^2/\alpha_V^2 = 1/30$, and keep the phase difference θ between the vertical and horizontal direction to be 0. Therefore, the expression of quantum fluctuations of Stokes operators can be obtained as follows:

$$\begin{aligned}\Delta^2 \hat{S}_0 &= \Delta^2 \hat{S}_1 = \alpha_V^2 \Delta^2 \hat{X}_V, \\ \Delta^2 \hat{S}_2 &= \alpha_V^2 \Delta^2 \hat{X}_H, \\ \Delta^2 \hat{S}_3 &= \alpha_V^2 \Delta^2 \hat{Y}_H.\end{aligned}\quad (13)$$

In the following, we couple the strong coherent light \hat{a}_{c1} , \hat{a}_{c2} , and \hat{a}_{c3} in the vertical polarization direction with the weak quadrature entangled optical fields \hat{a}_2 , \hat{a}_4 , and \hat{a}_5 in the

horizontal polarization direction on PBS1, PBS2, and PBS3, as shown in Fig. 1. Therefore, quadrature entanglement is transformed to Stokes operator entanglement, and we obtain the entanglement of the Stokes operator \hat{S}_{2x} , \hat{S}_{3x} , \hat{S}_{2y} , \hat{S}_{3y} , \hat{S}_{2z} , and \hat{S}_{3z} of three optical beams \hat{a}_x , \hat{a}_y , and \hat{a}_z . All four Stokes parameters can be easily measured by the polarization beam splitter, half-wave plate, and quarter-wave plate.

4. VERIFICATION OF CV THREE-COLOR POLARIZATION ENTANGLED OPTICAL FIELDS

Two methods are typically used to characterize the CV entanglement: one is inseparability criterion and the other is PPT criterion. The inseparability criterion is a sufficient condition for entanglement. In 2000, Duan first proposed the bipartite inseparability criterion for quadrature [32], and then van Loock and Furusawa generalized it to multipartite inseparability criterion for quadrature [33]. For tripartite entanglement, if the operator correlation variances satisfy the inequality $\langle \Delta(\hat{A}_i - \hat{A}_j)^2 \rangle + \langle \Delta(\sum_{i=1}^N \hat{B}_i)^2 \rangle < 4$ or $\langle \Delta(\sum_{i=1}^N \hat{A}_i)^2 \rangle + \langle \Delta(\sum_{i=1}^N \hat{B}_i)^2 \rangle < 4$ ($i, j = 1, 2, 3$), where \hat{A}_i and \hat{B}_i are the conjugate operators, a tripartite GHZ-like entangled state exists. According to the multipartite inseparability criterion in [33] and commutation relation of Stokes operators, we can obtain the tripartite inseparability criterion of Stokes operators for optical beams x, y, z , and we can define the normalized tripartite correlation variance of Stokes operators $I(\hat{S}_2, \hat{S}_3)$ as follows:

$$I_1(\hat{S}_2, \hat{S}_3) = \frac{\Delta^2(\hat{S}_{2y} - \hat{S}_{2z}) + \Delta^2(\hat{S}_{3x} + \hat{S}_{3y} + \hat{S}_{3z})}{2|[\hat{S}_2, \hat{S}_3]|}, \quad (14)$$

$$I_2(\hat{S}_2, \hat{S}_3) = \frac{\Delta^2(\hat{S}_{2x} - \hat{S}_{2y}) + \Delta^2(\hat{S}_{3x} + \hat{S}_{3y} + \hat{S}_{3z})}{2|[\hat{S}_2, \hat{S}_3]|}, \quad (15)$$

$$I_3(\hat{S}_2, \hat{S}_3) = \frac{\Delta^2(\hat{S}_{2x} - \hat{S}_{2z}) + \Delta^2(\hat{S}_{3x} + \hat{S}_{3y} + \hat{S}_{3z})}{2|[\hat{S}_2, \hat{S}_3]|}. \quad (16)$$

Thus, $I_i(\hat{S}_2, \hat{S}_3) < 1$ ($i = 1, 2, 3$) guarantees the quantum state of optical fields is inseparable. If any two inequalities in the set of inequalities are simultaneously satisfied, the three optical modes are a CV GHZ-like entangled state.

On the other hand, the PPT entanglement criterion proposed by Simon is the sufficient and necessary condition for the Gaussian state [34,35]. The entanglement properties of optical fields are related to the covariance matrix. The first-order moments are related to the average value, and the second-order moments correspond to the correlated matrix and entanglement. After applying the partial transposition operation to each subset, we obtain the partially transposed covariance matrix \tilde{V}_i ($i = x, y, z$). The smallest symplectic eigenvalue \tilde{v}_i ($i = x, y, z$) of each partially transposed covariance matrix is used to verify the entanglement, and, if $\tilde{v}_i < 1$, the state is entangled. Because of the interchangeability of signal and idler optical fields \hat{a}_y and \hat{a}_z from the NOPOII, their correlation variances are the same $I_2(\hat{S}_2, \hat{S}_3) = I_3(\hat{S}_2, \hat{S}_3)$, and their the smallest symplectic eigenvalues are equal $\tilde{v}_y = \tilde{v}_z$.

According to Eqs. (1) and (8), and taking the output optical field a_3 of NOPOI as the pump field of NOPOII, we can obtain the output quadrature entanglement of a cascaded NOPO

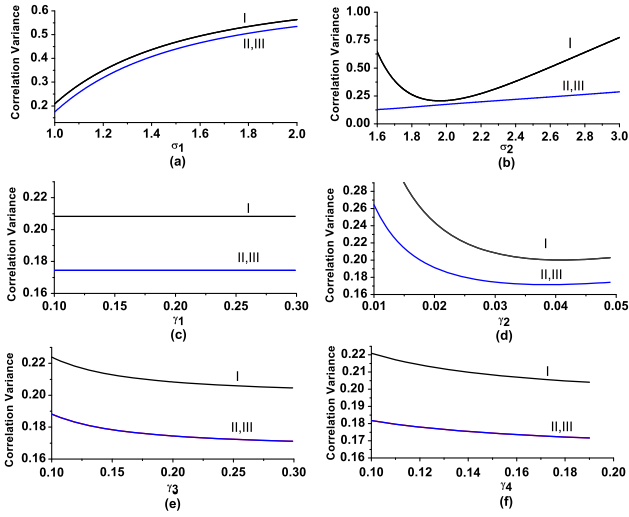


Fig. 2. Functions of correlation variance of \hat{S}_2 and \hat{S}_3 versus the parameters of cascaded NOPO system. (a) and (b) Pump power factor of NOPOI(II). (c) and (d) Pump input coupling transmissivity of NOPOI(II). (e) and (f) Signal (idler) output coupling transmissivity of NOPOI(II). Traces I, II, and III are for $I_1(\hat{S}_2, \hat{S}_3)$, $I_2(\hat{S}_2, \hat{S}_3)$, $I_3(\hat{S}_2, \hat{S}_3)$, respectively.

system. Using Eq. (13), the output polarization correlation results are obtained. Then, we are able to analyze the dependence of inseparability criterion and PPT criterion on each parameter, as shown in Figs. 2 and 3, respectively. In numerical calculation, we consider the analysis frequency 1 MHz. We take the pump input coupling transmissivity to be 0.20 for NOPOI(II). All the intracavity losses for pump, signal, and idler optical fields are considered as 0.001.

First, we will analyze the three-color polarization entanglement by inseparability criterion. Figure 2(a) shows the function of the correlation variance of Stokes operator $I_i(\hat{S}_2, \hat{S}_3)$ versus the pump power factor σ_1 of the NOPOI when we keep $\gamma_1 = 0.20$, $\gamma_2 = 0.03$, $\gamma_3 = 0.20$, $\gamma_4 = 0.15$, and $\sigma_2 = 2$. We can see that the correlation variance is smaller when the pump power is close to the threshold. Figure 2(b) shows the function of the correlation variance $I_i(\hat{S}_2, \hat{S}_3)$ versus the pump power factor σ_2 of the NOPOII while $\gamma_1 = 0.20$, $\gamma_2 = 0.03$, $\gamma_3 = 0.20$, $\gamma_4 = 0.15$, and $\sigma_1 = 1$ are kept. We can see that there is a minimum value of the correlation variance when the pump power factor is close to 2 for $I_1(\hat{S}_2, \hat{S}_3)$.

Figures 2(c) and 2(d) illustrate the functions of the correlation variance $I_i(\hat{S}_2, \hat{S}_3)$ versus the transmissivity of the pump input coupler of the NOPOI and NOPOII, as we keep $\gamma_2 = 0.03$, $\gamma_3 = 0.20$, $\gamma_4 = 0.15$, $\sigma_1 = 1$, $\sigma_2 = 2$, and $\gamma_1 = 0.20$, $\gamma_2 = 0.03$, $\gamma_4 = 0.15$, $\sigma_1 = 1$, and $\sigma_2 = 2$, respectively. Figures 2(e) and 2(f) demonstrate the functions of the correlation variance $I_i(\hat{S}_2, \hat{S}_3)$ versus the transmissivity of the signal (idler) output coupler of the NOPOI and NOPOII in the condition of $\gamma_1 = 0.20$, $\gamma_3 = 0.20$, $\gamma_4 = 0.15$, $\sigma_1 = 1$, $\sigma_2 = 2$, and $\gamma_1 = 0.20$, $\gamma_2 = 0.03$, $\gamma_3 = 0.20$, $\sigma_1 = 1$, and $\sigma_2 = 2$, respectively.

In the following, we will analyze the three-color polarization entangled state by PPT criterion, which has similar results to the inseparability criterion results. Figures 3(a) and 3(b)

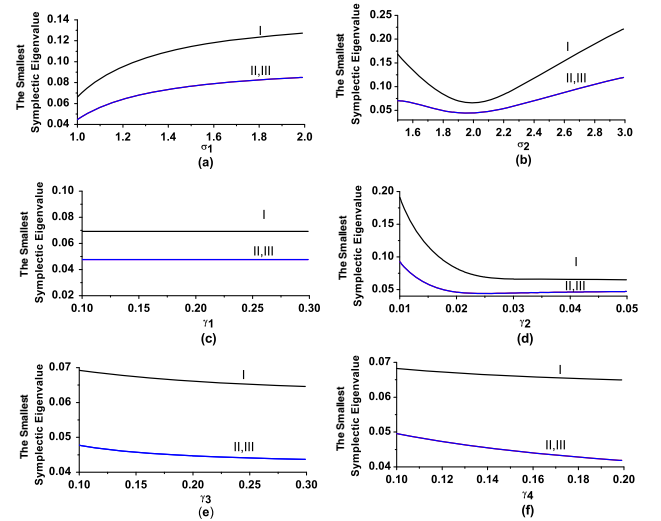


Fig. 3. Dependence of the smallest symplectic eigenvalue of \hat{S}_2 and \hat{S}_3 on the parameters of cascaded NOPO system. (a) and (b) Pump power factor of NOPOI(II). (c) and (d) Pump input coupling transmissivity of NOPOI(II). (e) and (f) Signal (idler) output coupling transmissivity of NOPOI(II). Traces I, II, and III are for \tilde{v}_x , \tilde{v}_y , \tilde{v}_z , respectively.

illustrate the dependence of the smallest symplectic eigenvalue of the partial transposition covariance matrix for the Stokes operator \hat{S}_2 and \hat{S}_3 of optical beams \hat{a}_x , \hat{a}_y , and \hat{a}_z on the pump power factor σ_1 and σ_2 of each NOPO when we keep $\gamma_1 = 0.20$, $\gamma_2 = 0.03$, $\gamma_3 = 0.20$, $\gamma_4 = 0.15$, $\sigma_2 = 2$, and $\gamma_1 = 0.20$, $\gamma_2 = 0.03$, $\gamma_3 = 0.20$, $\gamma_4 = 0.15$, and $\sigma_1 = 1$, respectively. We can see that the smallest symplectic eigenvalue is smaller when the pump power is close to the threshold for the NOPOI. There is a minimum value of the smallest symplectic eigenvalue when the pump power factor is close to 2. The dependence of the smallest symplectic eigenvalue on the transmissivity of the pump input coupler and the signal (idler) output coupler of each NOPO is drawn from Figs. 3(c) to 3(f). The results are also similar to those of the inseparability criterion.

The entanglement is not sensitive to γ_1 . For γ_3 , the entanglement degree will improve if the γ_3 are larger, and, when $\gamma_3 > 0.20$, the entanglement almost reaches the best case. However, the pump threshold power is high if the γ_1 and γ_3 are large. The cascaded system needs a high entanglement degree and low threshold power at the same time. Thus, we create a balance between the two factors and choose $\gamma_1 = \gamma_3 = 0.20$, according to the practical experimental condition.

For γ_2 and γ_4 , the entanglement degree is better when γ_2 and γ_4 are large because the ratio of entanglement output and noise output caused by intracavity loss is high. While $\gamma_2 > 0.03$, the entanglement almost reaches the best case. If $\gamma_4 > 0.15$, the criteria for the entanglement are satisfied and are not sensitive to γ_4 . The pump threshold power is high if the γ_2 and γ_4 are large. We need to consider the pump power of each NOPO and try to create a low pump threshold. Thus, we choose $\gamma_2 = 0.03$ and $\gamma_4 = 0.15$, and the entanglement almost reaches the optimal case, and the threshold is experimental reasonable.

For the phase quadrature, the correlation variance or the symplectic eigenvalue will increase if the normalized pump power factor of NOPOI is increased. Thus, for Stokes S2 and S3, the correlation variance or the symplectic eigenvalue will increase when the pump power of NOPOI is increased. We choose the $\sigma_1 = 1$.

The beams y and z are from NOPOII. If the pump power of NOPOII is close to threshold, there is multimode competition, and the correlation variance or the symplectic eigenvalue is high. The correlation variance or the symplectic eigenvalue will sharply decrease, when the power is increased. When the normalized pump power factor is near 2, there is a minimum value. After that point, the correlation variance or the symplectic eigenvalue will increase again. The correlation variance or the symplectic eigenvalue of the phase quadrature will increase when the normalized pump power factor is increased. We choose $\sigma_2 = 2$ near the minimum value.

We obtain the optimal values according to Figs. 2 and 3 by taking a differential calculation and other practical experimental conditions. Thus, we choose the optimal experimental parameters as $\gamma_1 = 0.20$, $\gamma_2 = 0.03$, $\gamma_3 = 0.20$, $\gamma_4 = 0.15$, $\sigma_1 = 1$, and $\sigma_2 = 2$.

The violation of inseparability criterion of light polarization is the sufficient condition of entanglement, and the violation of PPT criterion of light polarization is the necessary and sufficient condition of entanglement. We can use them as entanglement criteria and quality of entanglement. The boundary of normalized tripartite correlation variance of polarization is 1, and, if the normalized correlation variance is less than 1, the entanglement exists. From Fig. 2, we can see that it is much smaller than 1, and we obtain a three-color entanglement. The boundary of the smallest symplectic eigenvalue is 1, and, if the smallest symplectic eigenvalue is less 1, the entanglement exists. As illustrated in Fig. 3, it is less than 1, and three-color entanglement is verified.

The CV polarization entanglement is sensitive to loss. We will consider the dependence of entanglement on the intracavity loss. Figure 4 shows the normalized correlation variance and the smallest symplectic eigenvalue as a function of the intracavity loss of the signal optical beam for NOPOI. The normalized correlation variance and the smallest symplectic eigenvalue will increase when the loss is large. Even when the intracavity loss reaches 0.15, the entanglement does not exist.

We can choose the laser with the wavelength $\lambda_1 = 398$ nm to be the pump optical fields for NOPOI and produce the

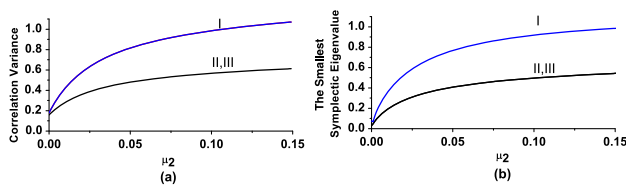


Fig. 4. (a) Dependence of the correlation variance of \hat{S}_2 and \hat{S}_3 on the intracavity loss of signal (idler) optical beam for NOPOI. Traces I, II, and III are for $I_1(\hat{S}_2, \hat{S}_3)$, $I_2(\hat{S}_2, \hat{S}_3)$, and $I_3(\hat{S}_2, \hat{S}_3)$, respectively. (b) Dependence of the smallest symplectic eigenvalue of \hat{S}_2 and \hat{S}_3 on the intracavity loss of signal (idler) optical beam for NOPOI. Traces I, II, and III are for \tilde{v}_x , \tilde{v}_y , and \tilde{v}_z , respectively.

entangled optical fields at wavelengths $\lambda_2 = 852$ nm and $\lambda_3 = 746$ nm by precisely controlling the temperature of NOPOI nonlinear crystal because of the capacity of frequency tuning. At the same time, the optical fields at wavelength λ_3 are used as pump optical fields for NOPOII to generate the entangled optical fields at wavelengths $\lambda_4 = 1550$ nm and $\lambda_5 = 1440$ nm by changing the temperature of NOPOII nonlinear crystal. The optical fields at wavelength $\lambda_2 = 852$ nm can correspond to the cesium atoms absorption line and can be used in quantum interface of atomic spin and light polarization. The optical fields at wavelengths $\lambda_4 = 1550$ nm and $\lambda_5 = 1440$ nm can match the fiber transmission window. This system can be applied in quantum memory and long-distance quantum communication for constructing quantum repeater and quantum networks [29].

5. CONCLUSION

In summary, we have theoretically proposed direct generation of CV three-color spatially separated GHZ-like polarization entangled optical fields by coupling the strong coherent light with the weak CV three-color quadrature entangled light derived from a cascaded NOPO system. According to inseparability criterion and PPT criterion, the dependencies of the correlation variance and the smallest symplectic eigenvalue of the partial transposition covariance matrix of the resulting CV three-color polarization entangled state on the pump power factor and the signal (idler) output coupling transmissivity of each NOPO are numerically calculated, and we may choose the optimal experimental parameters to provide direct reference for designing a practical system. This approach does not rely on the post-selection, and the wavelengths of the CV three-color polarization entangled optical fields can match the atomic absorption line and optical fiber transmission window due to the tuning capacity of NOPO, which can be applied in the future quantum information networks, and especially the interface between atomic spin and light polarization, quantum memory, quantum internet, and long-distance quantum communication.

Funding. National Natural Science Foundation of China (NSFC) (11304190, 11322440, 11474190).

REFERENCES

1. H. A. Bachor and T. C. Ralph, *A Guide To Experiments in Quantum Optics* (Wiley, 2004).
2. P. G. Kwiat, K. Mattle, H. Weinfurter, A. Zeilinger, A. V. Sergienko, and Y. Shih, "New high-intensity source of polarization-entangled photon pairs," *Phys. Rev. Lett.* **75**, 4337–4341 (1995).
3. X. C. Yao, T. X. Wang, P. Xu, H. Lu, G. S. Pan, X. H. Bao, C. Z. Peng, C. Y. Lu, Y. A. Chen, and J. W. Pan, "Observation of eight-photon entanglement," *Nat. Photonics* **6**, 225–228 (2012).
4. Z. Y. Ou, S. F. Pereira, H. J. Kimble, and K. C. Peng, "Realization of the Einstein–Podolsky–Rosen paradox for continuous variables," *Phys. Rev. Lett.* **68**, 3663–3666 (1992).
5. X. L. Su, Y. P. Zhao, S. H. Hao, X. J. Jia, C. D. Xie, and K. C. Peng, "Experimental preparation of eight-partite cluster state for photonic qumodes," *Opt. Lett.* **37**, 5178–5180 (2012).
6. H. J. Kimble, "The quantum internet," *Nature* **453**, 1023–1030 (2008).
7. H. Zhang, X. M. Jin, J. Yang, H. N. Dai, S. J. Yang, T. M. Zhao, J. Rui, Y. He, X. Jiang, F. Yang, G. S. Pan, Z. S. Yuan, Y. J. Deng, Z. B. Chen, X. H. Bao, S. Chen, B. Zhao, and J. W. Pan, "Preparation and storage of frequency-uncorrelated entangled photons from cavity-enhanced

- spontaneous parametric downconversion," *Nat. Photonics* **5**, 628–632 (2011).
8. Z. X. Xu, Y. L. Wu, L. Tian, L. R. Chen, Z. Y. Zhang, Z. H. Yan, S. J. Li, H. Wang, C. D. Xie, and K. C. Peng, "Long lifetime and high-fidelity quantum memory of photonic polarization qubit by lifting zeeman degeneracy," *Phys. Rev. Lett.* **111**, 240503 (2013).
 9. J. Appel, E. Figueroa, D. Korystov, M. Lobino, and A. I. Lvovsky, "Quantum memory for squeezed light," *Phys. Rev. Lett.* **100**, 093602 (2008).
 10. K. Honda, D. Akamatsu, M. Arikawa, Y. Yokoi, K. Akiba, S. Nagatsuka, T. Tanimura, A. Furusawa, and M. Kozuma, "Storage and retrieval of a squeezed vacuum," *Phys. Rev. Lett.* **100**, 093601 (2008).
 11. J. Cviklinski, J. Ortalo, J. Laurat, A. Bramati, M. Pinard, and E. Giacobino, "Reversible quantum interface for tunable single-sideband modulation," *Phys. Rev. Lett.* **101**, 133601 (2008).
 12. K. S. Choi, H. Deng, J. Laurat, and H. J. Kimble, "Mapping photonic entanglement into and out of a quantum memory," *Nature* **452**, 67–71 (2008).
 13. A. M. Marino, R. C. Pooser, V. Boyer, and P. D. Lett, "Tunable delay of Einstein–Podolsky–Rosen entanglement," *Nature* **457**, 859–862 (2009).
 14. M. Hosseini, G. Campbell, B. M. Sparkes, P. K. Lam, and B. C. Buchler, "Unconditional room-temperature quantum memory," *Nat. Phys.* **7**, 794–798 (2011).
 15. K. Jensen, W. Wasilewski, H. Krauter, T. Fernholz, B. M. Nielsen, M. Owari, M. B. Plenio, A. Serafini, M. M. Wolf, and E. S. Polzik, "Quantum memory for entangled continuous-variable states," *Nat. Phys.* **7**, 13–16 (2010).
 16. H. Hubel, D. Hamel, A. Fedrizzi, S. Ramelow, K. J. Resch, and T. Jennewein, "Direct generation of photon triplets using cascaded photon-pair sources," *Nature* **466**, 601–603 (2010).
 17. L. Shalm, D. Hamel, Z. Yan, C. Simon, K. Resch, and T. Jennewein, "Three-photon energy-time entanglement," *Nat. Phys.* **9**, 19–22 (2012).
 18. A. S. Villar, L. S. Cruz, K. N. Cassemiro, M. Martinelli, and P. Nussenzweig, "Generation of bright two-color continuous variable entanglement," *Phys. Rev. Lett.* **95**, 243603 (2005).
 19. X. L. Su, A. H. Tan, X. J. Jia, Q. Pan, C. D. Xie, and K. C. Peng, "Experimental demonstration of quantum entanglement between frequency-nondegenerate optical twin beams," *Opt. Lett.* **31**, 1133–1135 (2006).
 20. J. Jing, S. Feng, R. Bloomer, and O. Pfister, "Experimental continuous-variable entanglement from a phase-difference-locked optical parametric oscillator," *Phys. Rev. A* **74**, 041804 (2006).
 21. G. Keller, V. D'Auria, N. Treps, T. Coudreau, J. Laurat, and C. Fabre, "Experimental demonstration of frequency-degenerate bright EPR beams with a self-phase-locked OPO," *Opt. Express* **16**, 9351–9356 (2008).
 22. Y. M. Li, X. M. Guo, Z. L. Bai, and C. C. Liu, "Generation of two-color continuous variable quantum entanglement at 0.8 and 1.5 μm ," *Appl. Phys. Lett.* **97**, 031107 (2010).
 23. A. S. Villar, M. Martinelli, C. Fabre, and P. Nussenzweig, "Direct production of tripartite pump-signal-idler entanglement in the above-threshold optical parametric oscillator," *Phys. Rev. Lett.* **97**, 140504 (2006).
 24. A. S. Coelho, F. A. S. Barbosa, K. N. Cassemiro, A. S. Villar, M. Martinelli, and P. Nussenzweig, "Three-color entanglement," *Science* **326**, 823–826 (2009).
 25. A. H. Tan, C. D. Xie, and K. C. Peng, "Bright three-color entangled state produced by cascaded optical parametric oscillators," *Phys. Rev. A* **85**, 013819 (2012).
 26. X. J. Jia, Z. H. Yan, Z. Y. Duan, X. L. Su, H. Wang, C. D. Xie, and K. C. Peng, "Experimental realization of three-color entanglement at optical fiber communication and atomic storage wavelengths," *Phys. Rev. Lett.* **109**, 253604 (2012).
 27. D. Hamel, L. Shalm, H. Hubel, A. J. Miller, F. Marsili, V. B. Verma, R. P. Mirin, S. W. Nam, K. J. Resch, and T. Jennewein, "Direct generation of three-photon polarization entanglement," *Nat. Photonics* **8**, 801–807 (2014).
 28. N. Korolkova, G. Leuchs, R. Loudon, T. C. Ralph, and C. Silberhorn, "Polarization squeezing and continuous-variable polarization entanglement," *Phys. Rev. A* **65**, 052306 (2002).
 29. C. Peuntinger, B. Heim, C. R. Müller, C. Gabriel, C. Marquardt, and G. Leuchs, "Distribution of squeezed states through an atmospheric channel," *Phys. Rev. Lett.* **113**, 060502 (2014).
 30. W. Bowen, N. Treps, R. Schnabel, and P. Lam, "Experimental demonstration of continuous variable polarization entanglement," *Phys. Rev. Lett.* **89**, 253601 (2002).
 31. V. Josse, A. Dantan, A. Bramati, M. Pinard, and E. Giacobino, "Continuous variable entanglement using cold atoms," *Phys. Rev. Lett.* **92**, 123601 (2004).
 32. L. M. Duan, G. Giedke, J. I. Cirac, and P. Zoller, "Inseparability criterion for continuous variable systems," *Phys. Rev. Lett.* **84**, 2722–2725 (2000).
 33. P. van Loock and A. Furusawa, "Detecting genuine multipartite continuous-variable entanglement," *Phys. Rev. A* **67**, 052315 (2003).
 34. R. Simon, "Peres–Horodecki separability criterion for continuous variable systems," *Phys. Rev. Lett.* **84**, 2726–2729 (2000).
 35. R. F. Werner and M. M. Wolf, "Bound entangled Gaussian states," *Phys. Rev. Lett.* **86**, 3658–3661 (2001).